

Zr-2.5%Nb**DHC and fracture toughness behavior along the cracking direction in Zr-2.5%Nb pressure tube materials**

*, , ,

150

Zr-2.5%Nb

DHC

(T-L)

(T-R)

three point bend

60ppm

DHC

. DHC

,

(T-L)

250°C

DHC

2

.

T-L

T-R

DHC

250°C

three point bend

,

T-R

dj/da

T-L

40%

.

DHC

DHC

가

.

Abstract

To investigate the reason for the anisotropy of delayed hydride cracking (DHC) behavior in the longitudinal and radial directions in Zr-2.5%Nb pressure tube materials, two series of specimens of which cracking directions are the radial (T-R) and the longitudinal (T-L) one were machined and were hydrated with 60 ppm, and then DHC and fracture tests were carried out. The DHC results show that DHC velocity in the T-L specimens is two times faster than that of T-R specimens at 250°C, as reported earlier. Even though cracking direction is identical except cracking direction, the fact showing the anisotropy of DHC behavior suggests that DHC process is not controlled only by precipitation of hydride but may be controlled by the directional fracture behavior. The fracture test results shows that the dJ/da of T-R specimens is about 40% higher than that of T-L at RT and 250°C. This seems to be due to the difference in deformation mechanisms during fracture processes. Thus, the reason for the anisotropy of DHC seems be due to the difference in deformation mechanisms operated during cracking process along the cracking direction, namely, due to the difference in texture.

1.

Zr-2.5%Nb

DHC

가 CT

CB

DHC

[1, 2].

DHCV

DHCV

2

Fig. 1

DHC

(K_{IH})

DHC

Fig. 2[2-7]

K_{IH}가 50%
CT CB

, CB

CT

DHC

Zr-2.5%Nb

K_{IH}

가

[3].

(F)

(1-F)

DHC

가

$$K_{IH} = K_{IC \text{ of ductile matrix}} \times (1 - F) + K_{IC \text{ of brittle hydride}} \times F$$

(1)

K_{IH}가

가

Coleman

[8].

DHC

[9].

가

가

CB

가

DHC

three point bend

DHC

2.

DHC

three point bend

Zr-2.5%Nb

10%

가

가

-Zr

-Zr

400

72

가

60 ppm

300 96

Fig. 3 가 DHC (T-L) (T-R)
three point bend

(b) (W) 4mm DHCV ,
on-line 가
computer
25 250 가 가
DC potential drop
J-integral vs

Three point bend
XRD

3. DHCV Fig. 4
DHCV 2 가
가

CB DHC Fig. 5 6 CT
CT CB (1012) 가
(1012) (1121) 가
가
(1012) 가 30° (1121)
가 90° 가
(1012) 가
DHC DHC DHC K_{IH}
가 DHC

(1) K_{IH}
 (K_I)
 (K_I)
 DHC

Three point bend
 Fig. 7

250
 DHC
 가
 가 250

가

J-integral -
 CT
 (W = 4mm)
 1mm
 dJ/da T-L 40%

Fig. 8
 mm
 T-R
 DHC

60 ppm 250
 60 ppm
 250C three point bend
 가

170-250
 가

Fig. 9

1) DHC , 2)
 가 , 3)
 가 , 4) dj/da 40%

DHC
 K_{IH} DHCV
 [10].
 DHC

4.

- 1) DHC 2
- 2) DHC 가 (1012)
- 3) (1012) 가 (1121) 가 three point bend T-R dj/da 40%
- 4) DHC DHC

References

1. S. Sagat, C. E. Coleman, M. Griffiths, and B. J. S. Wilkins, Zirconium in the Nuclear Industry, Tenth International Symposium, ASTM STP 1245, 1994, pp. 35 -61.
2. S. S. Kim, S. C. Kwon, K. N. Choo, Y. M. Cheong, and Y. S. Kim, Key Engineering Materials, Vol. 183 -187 (2000) pp. 845 -850.
3. S. S. Kim, S. C. Kwon, and Y. S. Kim, J. Nucl. Mater. Vol. 273, 1999, pp.52 -59.
4. C. E. Coleman, S. Sagat, and K. F. Amouzouvi, Control of Microstructure to Increase the Tolerance of Zirconium Alloys to Hydride Cracking, Atomic Energy of Canada Limited Report AECL -9524 (1987).
5. C. E. Coleman, Zirconium in the Nuclear Industry, Fifth Conference, ASTM STP 754, 1982, pp. 393 -411.
6. H. Huang, and W. J. Mills, Metal. Transactions 22A (1991), pp.2149 -2060.
7. W. J. Mills, and F. H. Huang, Eng. Frac. Mech. 39 (1991), pp. 241 -257.
8. C. E. Coleman, B. A. Cheadle, C. D. Cann, and J. R. Theaker, Zirconium in the Nuclear Industry, Eleventh International Symposium, ASTM STP 1295, 1996, pp. 884 -898.
9. S. S. Kim, S. C. Kwon, K. N. Choo, Y. M. Cheong, and Y. S. Kim, Canadian Nuclear Society, 2000 Spring, Toronto, Canada
10. Y. S. Kim, Y. G. Matvienko, Y. M. Cheong, S. S. Kim, S. C. Kwon, Journal of Nuclear Materials, Vol. 278 (2000) pp. 251 -257.

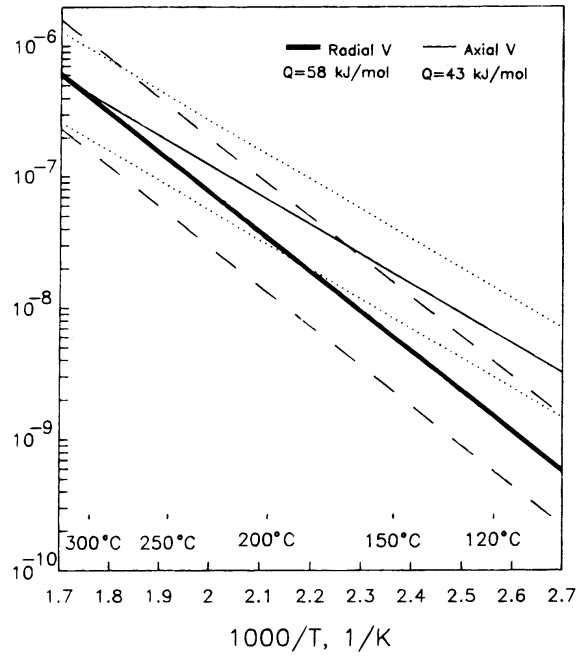


Fig. 1. Comparison of DHC velocity in the radial and longitudinal direction [1].

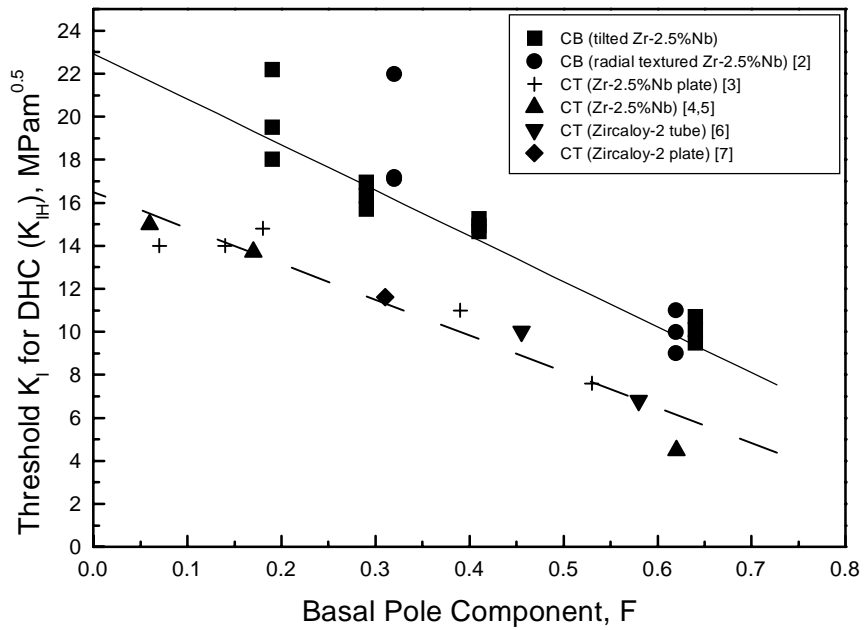


Fig. 2. Comparisons of K_{IH} measured from CT and CB specimens with the basal pole components in Zircaloy-2 and Zr-2.5%Nb materials [2-7].

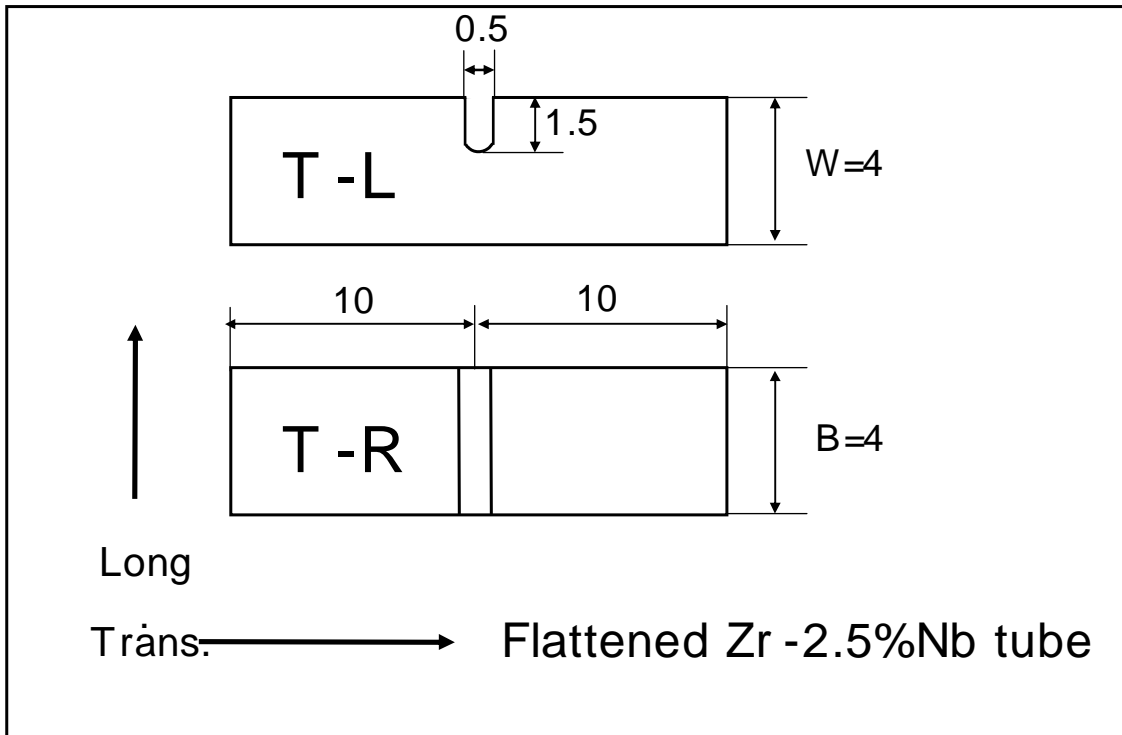


Fig. 3. Schematic illustration of dimension and configuration of three point bend specimens.

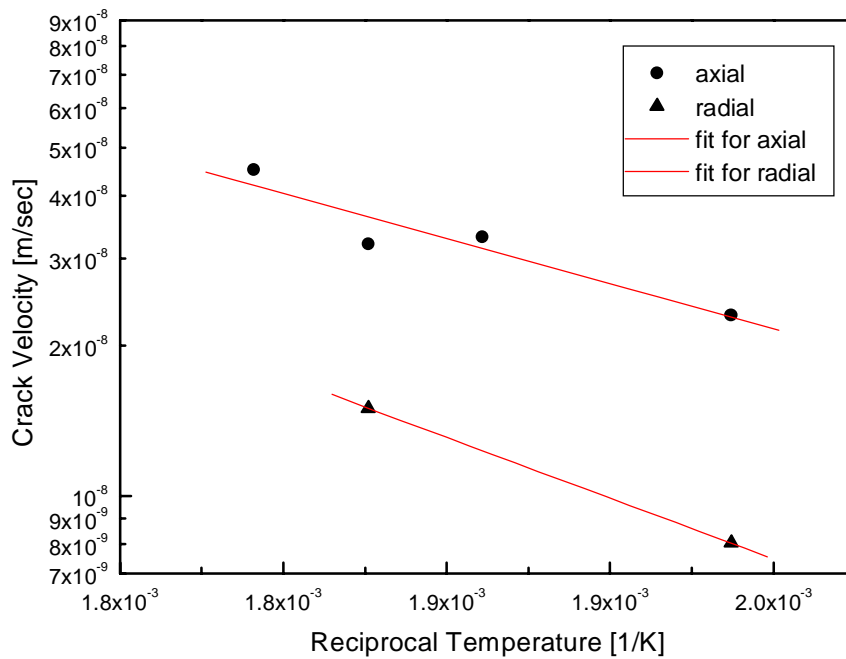


Fig. 4. DHC crack velocity in the T-L and T-R specimens with reciprocal temperature.

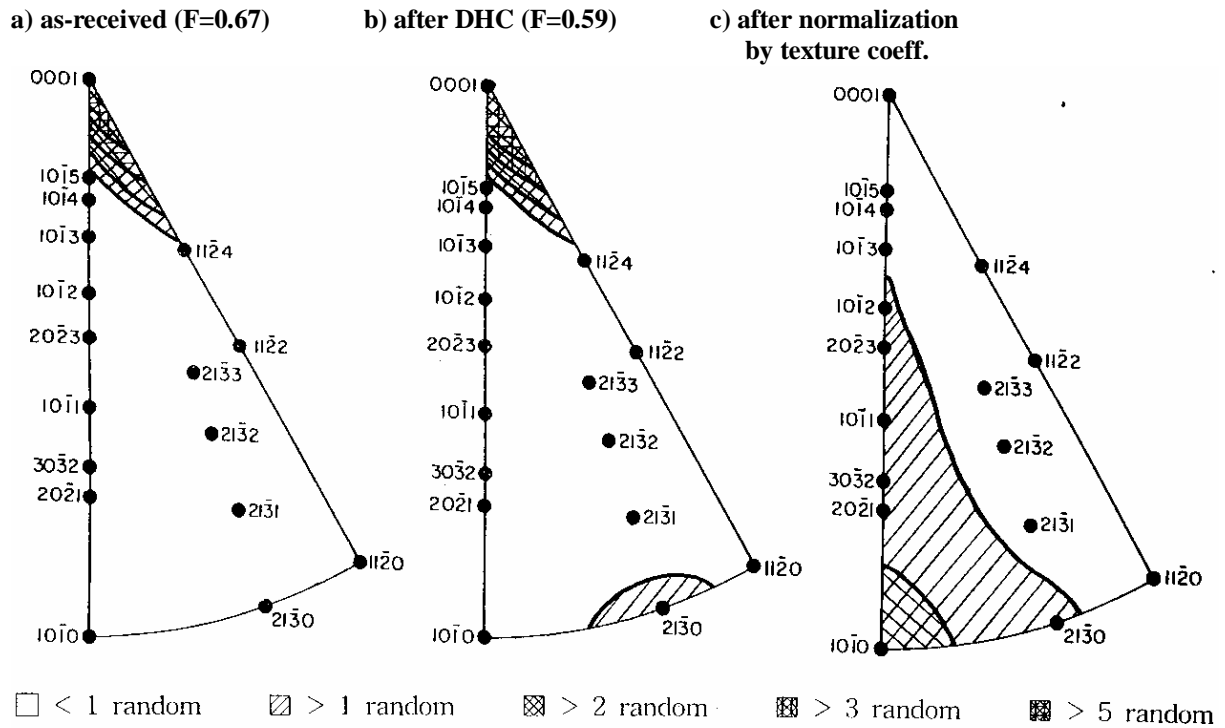


Fig. 5. Comparison of inverse pole figures for CT specimen before and after DHC in the longitudinal direction.

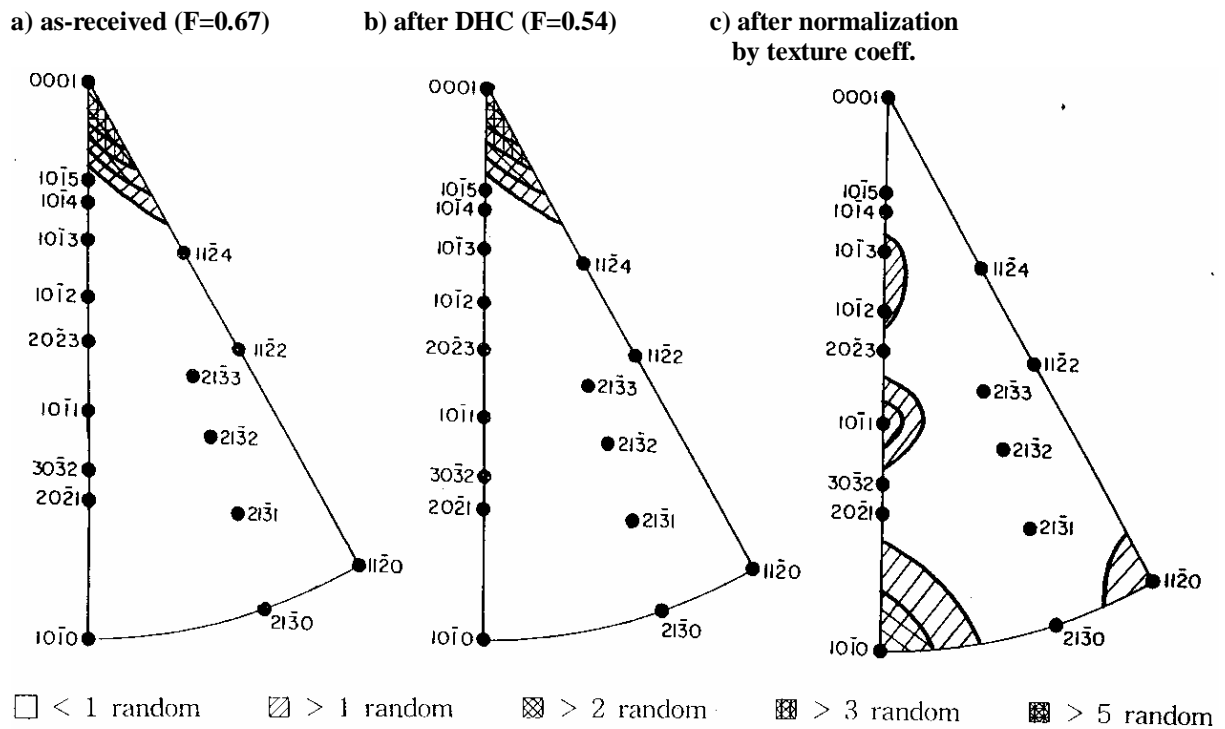


Fig. 6. Comparison of inverse pole figures for CB specimens before and after DHC in the radial direction.

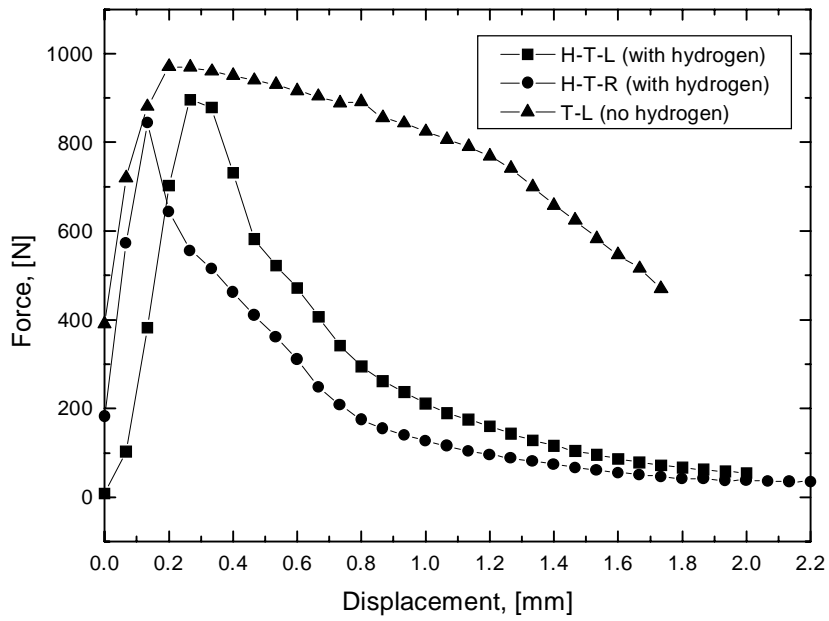


Fig. 7. Force-displacement curves for T-L and T-R specimens with and without hydrogen at RT.

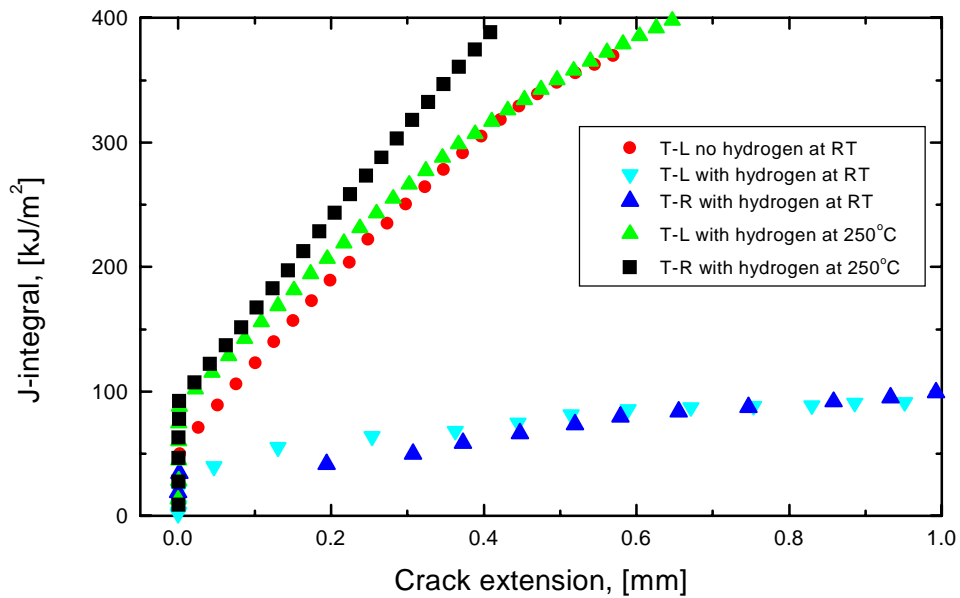


Fig. 8. Comparisons of J-integral and crack extension curves for T-R and T-L specimens at RT and 250°C.